10.24425/acs.2024.153098

Archives of Control Sciences
Volume 34(LXX), 2024
No. 4, *pages* 697–713

A new chaotic hyperjerk system with four quadratic nonlinearities, its bifurcation analysis, multistability, circuit design and complete synchronization design via active backstepping control

Sundarapandian VAIDYANATHAN, Aceng SAMBAS, Irene M. MOROZ, Chittineni ARUNA, Mohamad Afendee MOHAMED and Arun SUNDARAM

In this research work, we propose a new four-dimensional chaotic hyperjerk system with four quadratic nonlinearities. We carry out a detailed bifurcation analysis and derive conditions for the existence of a Hopf bifurcation for the new hyperjerk system. A linear analysis shows that there is only a unique trivial equilibrium state, whose stability depends solely on the parameter p. The only bifurcation possible is a Hopf bifurcation when $p = 2$. This is verified from bifurcation transition diagrams. We derive new results showing multistability and the existence of coexisting attractors for the new chaotic hyperjerk system. Using MultiSim, a new electronic circuit is designed for the new chaotic hyperjerk system with four quadratic nonlinearities. Finally, we

S. Vaidyanathan (corresponding author, e-mail: sundar@veltech.edu.in) is with Centre for Control Systems, Vel Tech University, 400 Feet Outer Ring Road, Avadi, Chennai-600062, Tamil Nadu, India and Faculty of Information and Computing, Universiti Sultan Zainal Abidin, Terengganu, Malaysia.

A. Sambas (e-mail: acengs@umtas.ac.id) is with Faculty of Informatics and Computing, Universiti Sultan Zainal Abidin, Gong Badak, 21300, Terengganu, Malaysia and Department of Mechanical Engineering, Universitas Muhammadiyah Tasikmalaya, Jawa Barat 46196, Indonesia.

Irene M. Moroz (e-mail: Irene.Moroz@maths.ox.ac.uk) is with Mathematical Institute, University of Oxford, Andrew Wiles Building, ROQ, Oxford Ox2 6GG, UK.

C. Aruna (e-mail: aruna.cse@kitsguntur.ac.in) is with Department of Computer Science and Engineering, KKR & KSR Institute of Technology and Sciences, Vinjanampadu, Vatticherukuru Mandal, Guntur-522017, Andhra Pradesh, India.

M.A. Mohamed (e-mail: mafendee@unisza.edu.my) is with Faculty of Information and Computing, Universiti Sultan Zainal Abidin, Terengganu, Malaysia.

A. Sundaram (e-mail: draruns@jerusalemengg.ac.in) is with Department of Electronics and Communication Engineering, Jerusalem College of Engineering, Narayanapuram, Pallikaranai, Chennai – 600 100, Tamil Nadu, India.

Received 28.03.2024.

present a control application for the proposed chaotic hyperjerk system with four quadratic nonlinearities. Using active backstepping control, we design a new controller that achieves complete synchronization for the master-slave chaotic hyperjerk systems with four quadratic nonlinearities.

Key words: chaotic systems, chaos, hyperjerk systems, bifurcation analysis, circuit design, backstepping control, synchronization

1. Introduction

Chaos theory has several applications in engineering and science branches such as lasers [1, 2], oscillators [3, 4], robots [5, 6], memristors [7, 8], cryptosystems [9, 10], financial systems [11, 12], etc.

In mechanical systems, a fourth-order autonomous hyperjerk differential equation is defined by the equation

$$\frac{\mathrm{d}^4 y}{\mathrm{d}t^4} = f\left(y, \frac{\mathrm{d}y}{\mathrm{d}t}, \frac{\mathrm{d}^2 y}{\mathrm{d}t^2}, \frac{\mathrm{d}^3 y}{\mathrm{d}t^3}\right). \tag{1}$$

If $y(t)$ stands for the displacement of a body, then $\dfrac{\mathrm{d}y}{\mathrm{d}t}$ stands for the velocity of the body and $dfrac\mathrm{d}^2 y\mathrm{d}t^2$ stands for the acceleration of the body. Furthermore, $\dfrac{\mathrm{d}^3 y}{\mathrm{d}t^3}$ stands for the jerk of the body and $\dfrac{\mathrm{d}^4 y}{\mathrm{d}t^4}$ stands for the hyperjerk of the body. This is the mechanical interpretation for the hyperjerk differential equation (1).

For dynamic analysis, it is convenient to express the fourth order autonomous ODE (1) as a system of equations as follows:

$$\begin{cases} \dot{y}_1 = y_2\,, \\ \dot{y}_2 = y_3\,, \\ \dot{y}_3 = y_4\,, \\ \dot{y}_4 = f(y_1, y_2, y_3, y_4). \end{cases} \tag{2}$$

In the hyperjerk system (2), $y_1 = y$, $y_2 = \dot{y}$, $y_3 = \ddot{y}$ and $y_4 = \dddot{y}$.

Hyperjerk systems have several applications in engineering such as image encryption [13], circuit design [14], memristors [15], robotics [16], etc.

In this research work, we propose a new four-dimensional chaotic hyperjerk system with four quadratic nonlinearities. Using Lyapunov exponents, and Kaplan dimension, we derive new results that the proposed hyperjerk system is a dissipative chaotic system with fractal Kaplan dimension.

We carry out a detailed bifurcation analysis and derive conditions for the existence of a Hopf bifurcation for the new hyperjerk system. Multistability of chaotic systems is a complex phenomenon that refers to the coexistence of several

chaotic or periodic attractors for the underlying system for same set of parameter values but different sets of initial states [17, 18]. We derive new results showing multistability for the new chaotic hyperjerk system.

Using MultiSim, a new electronic circuit is designed for the new chaotic hyperjerk system with four quadratic nonlinearities. Electronic circuit designs of chaotic systems are very useful for the real-world engineering applications of the systems [19, 20].

Finally, we present a control application for the proposed chaotic hyperjerk system with four quadratic nonlinearities. Using active backstepping control, we design a new controller that achieves complete synchronization for the master-slave chaotic hyperjerk systems with four quadratic nonlinearities.

2. A new chaotic hyperjerk system with four quadratic nonlinear terms

In this research work, we propose a new 4-D hyperjerk system with the dynamics

$$\begin{cases} \dot{x} = y, \\ \dot{y} = z, \\ \dot{z} = w, \\ \dot{w} = -x - y - pz - w - axz - bxy - cyz + qz^2 . \end{cases} \tag{3}$$

We use the notation X to represent the 4-D state (x, y, z, w) of the new hyperjerk system (3), which has four quadratic nonlinear terms.

We shall establish that the system (3) has a dissipative chaotic attractor for the parameter values

$$a = 0.3, \quad b = 0.2, \quad c = 0.4, \quad p = 0.2, \quad q = 0.2. \tag{4}$$

The Lyapunov exponents of the 4-D hyperjerk system (3) are found using MATLAB algorithm for the parameter values (4) and initial state $X(0) = (0.5, 0.3, 0.5, 0.3)$ as given below:

$$L_1 = 0.1831, \quad L_2 = 0, \quad L_3 = -0.1459, \quad L_4 = -1.0375. \tag{5}$$

Thus, the proposed hyperjerk system (3) has a dissipative and chaotic attractor.

Furthermore, the Kaplan dimension of the 4-D chaotic hyperjerk system (3) is attained as

$$D_L = 3 + \frac{L_1 + L_2 + L_3}{|L_4|} = 3.0359 \tag{6}$$

which exhibits the complexity of the proposed hyperjerk system (3).

To calculate the equilibrium points of the proposed hyperjerk system (3), we solve the equations $\dot{x} = 0$, $\dot{y} = 0$, $\dot{z} = 0$ and $\dot{w} = 0$. A simple calculation shows that $P_0 = (0, 0, 0, 0)$ is the unique equilibrium point of the 4-D hyperjerk system (3).

The Jacobian matrix of the 4-D hyperjerk system (3) at P_0 is found to be

$$J_0 = \begin{bmatrix} 0 & 1 & 0 & 0 \\ 0 & 0 & 1 & 0 \\ 0 & 0 & 0 & 1 \\ -1 & -1 & -p & -1 \end{bmatrix}. \tag{7}$$

The characteristic equation associated with J_0 is given by

$$s^4 + ps^3 + s^2 + s + 1 = 0. \tag{8}$$

Using the Routh array test, it can be easily established that the characteristic equation (8) will be *stable* if and only if $p > 2$.

For the chaotic case (4), $p = 0.2 < 2$. Hence, the characteristic equation (8) is unstable in the chaotic case. In fact, the eigenvalues of the matrix J_0 are computed as

$$\alpha_{1,2} = 0.4659 \pm 0.8848\mathrm{i}, \quad \alpha_{3,4} = -0.9659 \pm 0.2589\mathrm{i}. \tag{9}$$

This calculation shows that the proposed hyperjerk system (8) has an unstable, saddle-focus equilibrium at $P_0 = (0, 0, 0, 0)$.

Figure 1 shows the MATLAB signal plots of the proposed hyperjerk system (8) for the parametric values given by (4) and $X(0) = (0.5, 0.3, 0.5, 0.3)$.

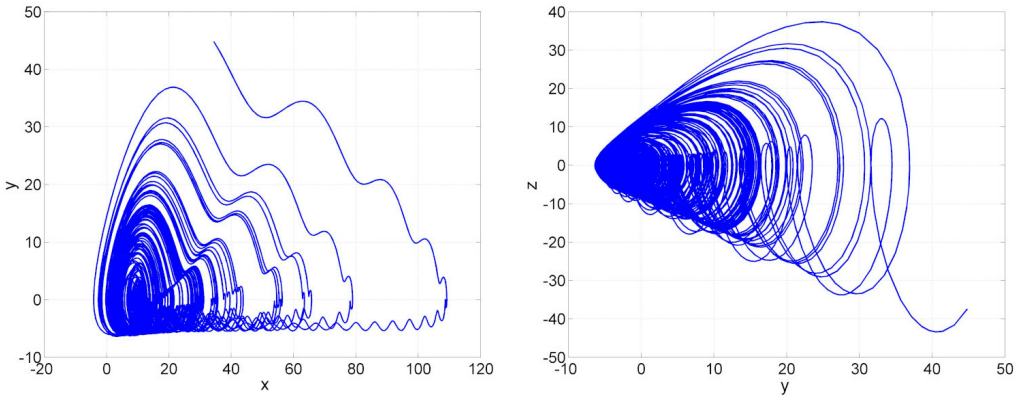

(a) (x, y) plot (b) (y, z) plot

Figure 1: (a), (b)

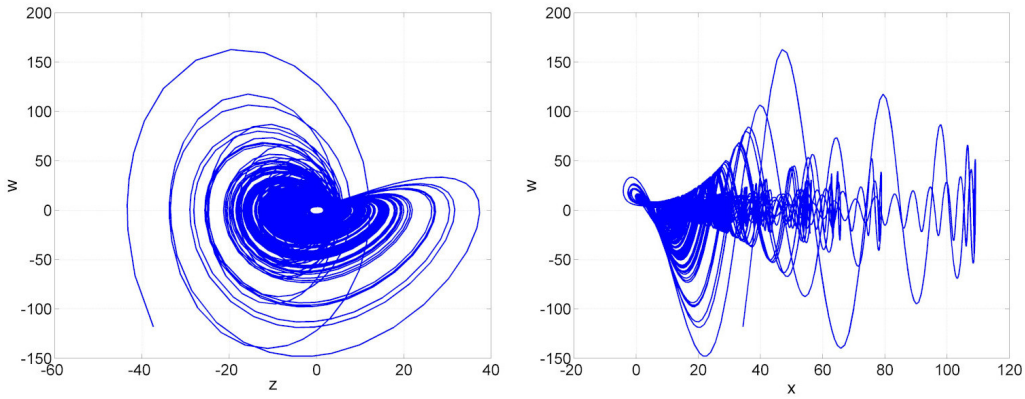

(c) (z, w) plot (d) (x, w) plot

Figure 1: MATLAB signal plots of the proposed hyperjerk system (3) for the parametric values given by (4) and $X(0) = (0.5, 0.3, 0.5, 0.3)$

3. Bifurcation analysis of the new chaotic hyperjerk system

The characteristic equation given in (8) for the linearization of the new chaotic hyperjerk system (3) depends only upon the parameter p. A Hopf bifurcation is possible, which can be shown by taking $s = \pm i\omega$ and equating real and imaginary parts to get

$$\omega^4 - p\omega^2 + 1 = 0, \qquad \omega^2 = 1. \tag{10}$$

This is satisfied when $p = 2$.

The remaining two eigenvalues of the characteristic equation (8) satisfy $s = -\frac{1}{2} \pm \frac{\sqrt{3}i}{2}$, which shows that the Hopf bifurcation is stable. This is clearly demonstrated in the bifurcation transition diagrams shown in Figure 2. To produce these plots, we initiated the integration at $p = 0.2$, using the initial data $(0.5, 0.3, 0.5, 0.3)$. We integrated for $500s$, discarding the first $300s$ as transients. Then the final condition was taking as the starting point for the next integration. The lower panel shows a regime of period-doubling bifurcations for $1.49 < p < 2$. There is a periodic orbit in $1.72 < p < 2$, which undergoes a period-doubling bifurcation at $p \approx 1.72$ to a period-2 orbit, which then loses stability at to a period-4 orbit at $p \approx 1.64$. There is a region of chaos until $p \approx 1.59$, followed by regions of chaotic and regular dynamics until a sudden enlargement of the chaotic regime at $p \approx 1.49$.

Figure 3 shows four phase portraits of (x, y) from this blown up region, showing a periodic orbit when $p = 1.8$, a period-2 orbit for $p = 1.7$, a period-4 orbit for $p = 1.63$ and a broad-banded period-5 orbit for $p = 1.58$.

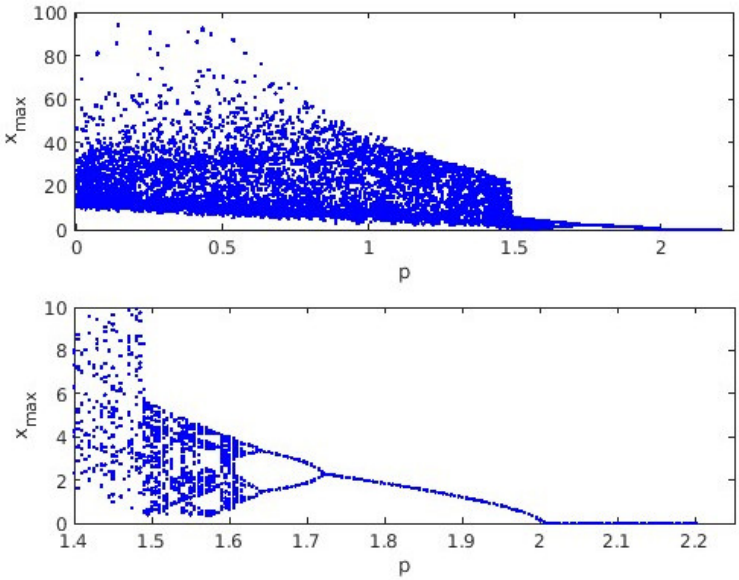

Figure 2: The bifurcation transition plots of $x_{\max}$ as p increases and decreases from $p = 0.2$ in $[0, 2.25]$, with initial conditions $(0.5, 0.3, 0.5, 0.3)$. We take the final data value as the initial data for the next increment/decrement. The upper panel shows the entire integration region, while the lower panel shows a blow-up of the period-doubling region for $1.49 < p < 2$. The Hopf bifurcation at $p = 2$ is clearly shown

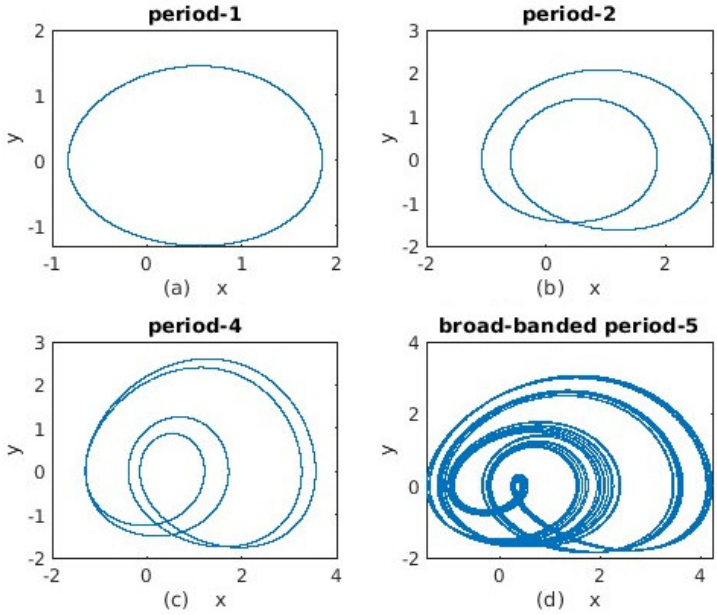

Figure 3: Phase portraits of (x, y) for (a) $p = 1.8$ (periodic orbit); (b) $p = 1.7$ (period-2 orbit); (c) $p = 1.63$ (period-4 orbit); (d) $p = 1.58$ (a broad-banded period-5 orbit)

4. Multistability in the new 4-D chaotic hyperjerk system

Multistability of chaotic systems is a complex phenomenon that refers to the coexistence of several chaotic or periodic attractors for the underlying system for same set of parameter values but different sets of initial states [17, 18]. We derive new results showing multistability for the new chaotic hyperjerk system (3).

In order to study the coexistence of attractors for the chaotic hyperjerk system (3) better, it is necessary to give some disturbance to the initial conditions under the condition of keeping the system parameters constant.

Figure 4 shows the dynamic behavior with coexistence of chaotic attractors with initial states $X_0 = (0.5, 0.3, 0.5, 0.3)$ (blue orbit) and $Y_0 = (-0.2, 0.2, -0.20.2)$ (red orbit).

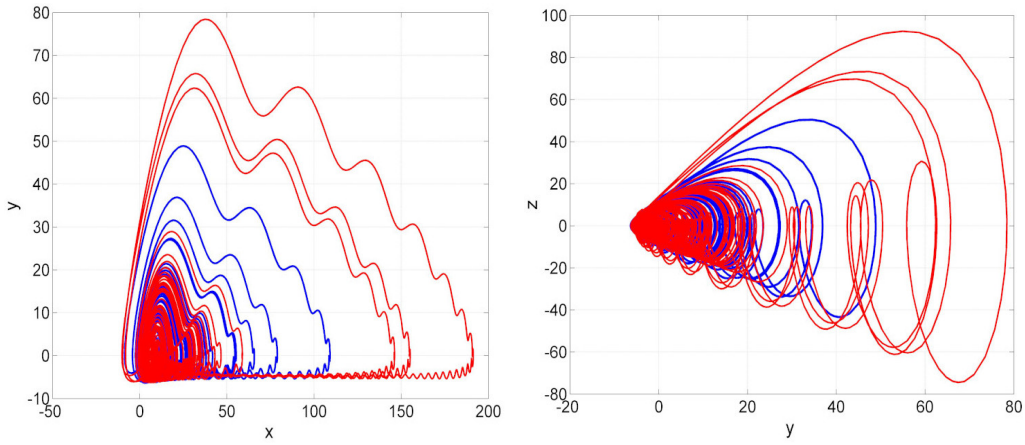

(a) (x, y) plot (b) (y, z) plot

Figure 4: Coexistence of two chaotic attractors of the hyperjerk system (3) with different initial values: the blue for $X_0 = (0.5, 0.3, 0.5, 0.3)$ and the red for $Y_0 = (-0.2, 0.2, -0.2, 0.2)$

5. Circuit design of the new chaotic hyperjerk system

In this segment, we create an electronic circuit employing Multisim software to implement the novel hyperjerk chaotic system. Utilizing Multisim, we combine TL082CD Op-amp, AD633JN multiplier, resistors, and capacitors to simulate the chaotic attractor. The schematic representation of the electronic circuit is illustrated in Figure 5, with x, y, z and w denoting the voltages across capacitors C_1, C_2, C_3, and C_4, respectively.

The electronic circuit for implementing the new hyperjerk system (3) is synthesized, as depicted in Figure 5. The equations governing the circuit are formulated

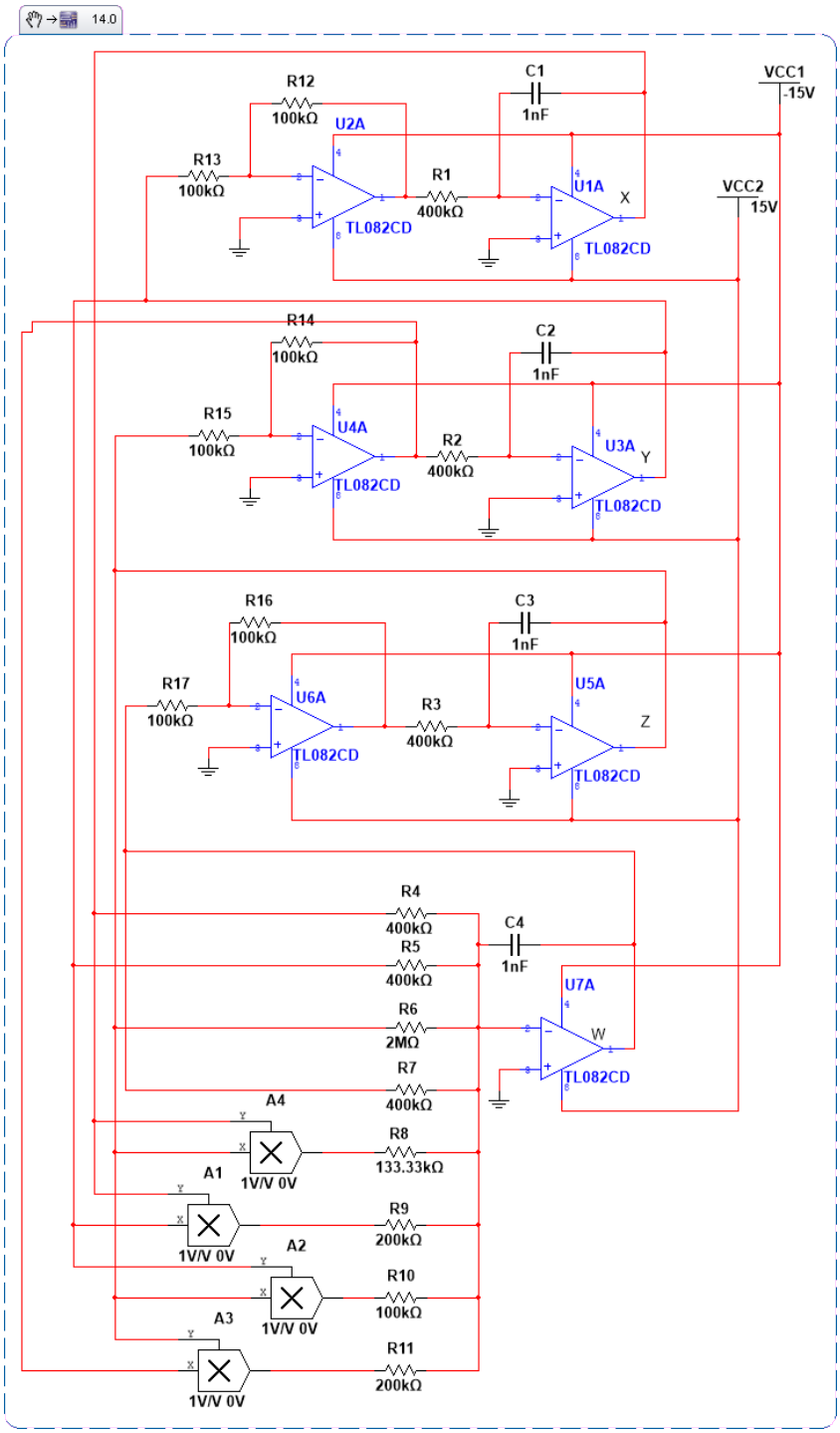

Figure 5: Electronic circuit of the Hyperjerk system using MultiSim 14.0

as follows:

$$\begin{cases} C_1\dot{x} = \dfrac{1}{R_1}y, \\ C_2\dot{y} = \dfrac{1}{R_2}z, \\ C_3\dot{z} = \dfrac{1}{R_3}w, \\ C_4\dot{w} = -\dfrac{1}{R_4}x - \dfrac{1}{R_5}y - \dfrac{1}{R_6}z - \dfrac{1}{R_7}w - \dfrac{1}{10R_8}xz \\ \qquad\quad - \dfrac{1}{10R_9}xy - \dfrac{1}{R_{10}}yz + \dfrac{1}{10R_11}z^2. \end{cases} \tag{11}$$

Here, x, y, z and w are the output voltages of the operational amplifiers U1A, U3A, U5A, and U7A, respectively. The values of circuit components are selected as: $R_1 = R_2 = R_3 = R_4 = R_5 = R_7 = 400$ kΩ, $R_6 = 2$ MΩ, $R_8 = 133.33$ kΩ, $R_9 = R_{11} = 200$ kΩ, $R_{10} = R_{12} = R_{13} = R_{14} = R_{15} = R_{16} = R_{17} = 100$ kΩ, $C_1 = C_2 = C_3 = C_4 = 1$ nF.

The phase portraits of the system (3) are visually depicted in Figures 6–9 through oscilloscope graphics. It is evident that the circuit simulation results

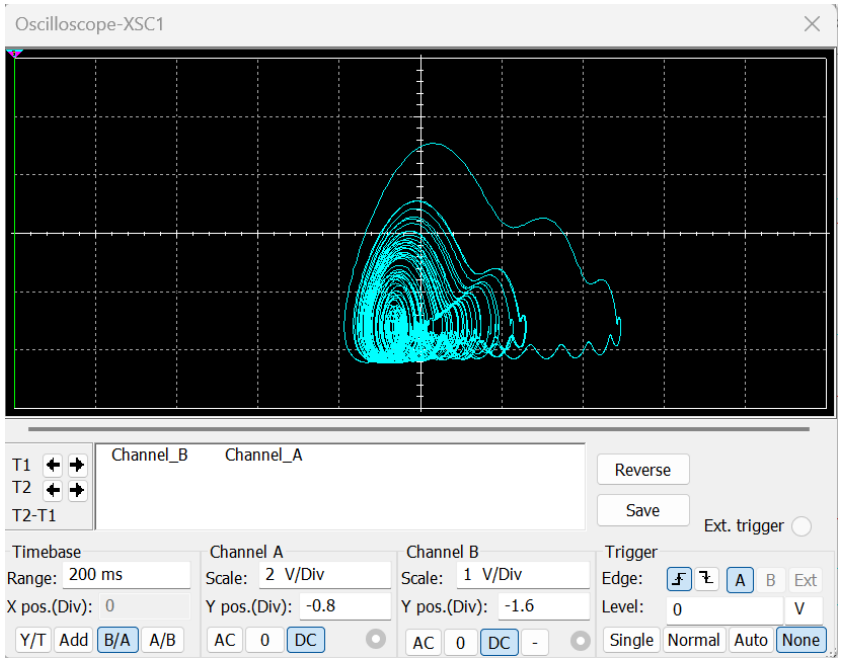

Figure 6: Oscilloscope output of the chaotic attractor of novel chaotic hyperjerk system in (x, y)-plane using MultiSim 14.0

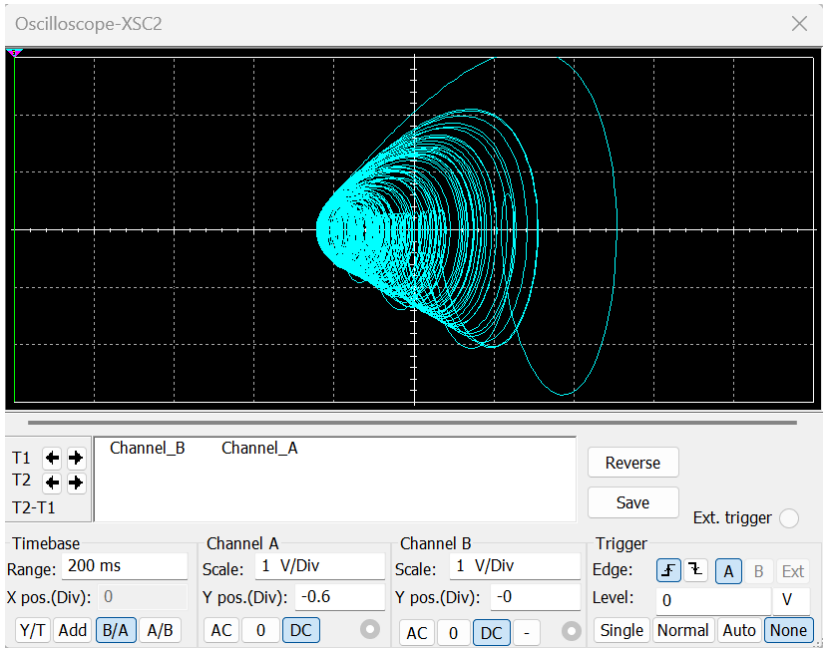

Figure 7: Oscilloscope output of the chaotic attractor of novel chaotic hyperjerk system in (y, z)-plane using MultiSim 14.0

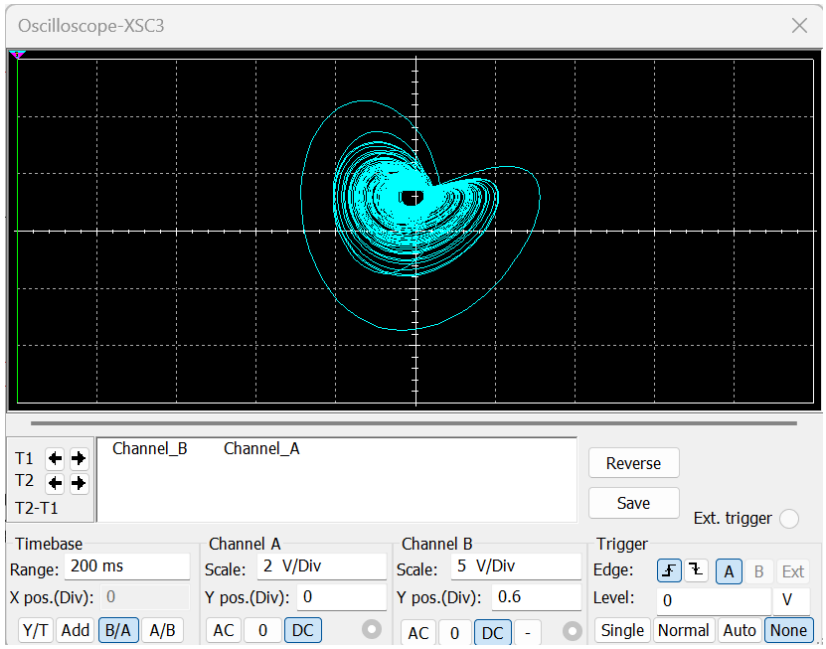

Figure 8: Oscilloscope output of the chaotic attractor of novel chaotic hyperjerk system in (z, w)-plane using MultiSim 14.0

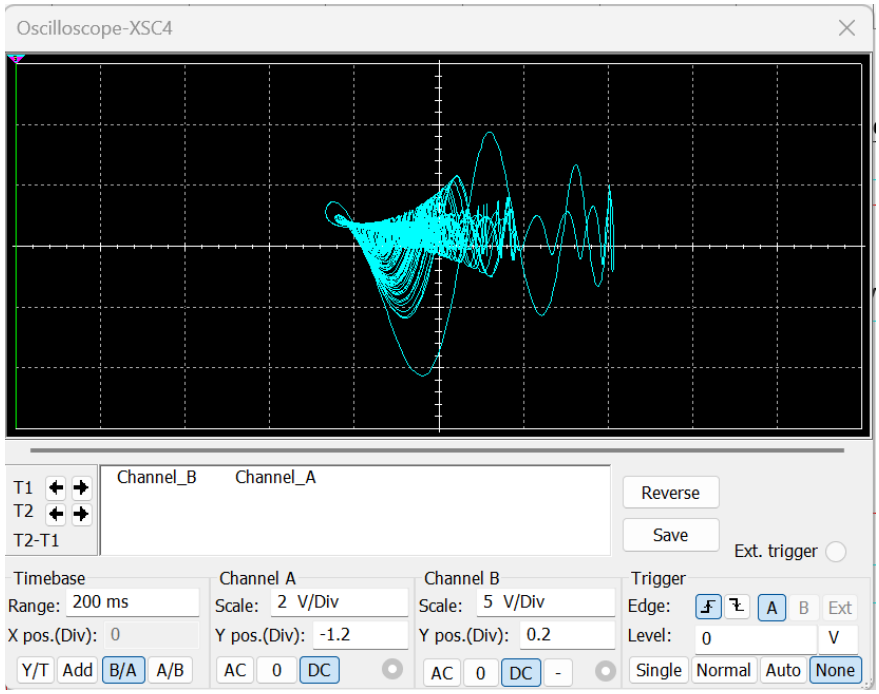

Figure 9: Oscilloscope output of the chaotic attractor of novel chaotic hyperjerk system in (x, w)-plane using MultiSim 14.0

of the oscilloscope graphics presented in Figures 6–9 align with the MATLAB simulation results provided in Figure 1.

6. Active backstepping synchronization of the new chaotic hyperjerk systems

Here, we shall deploy active backstepping control for globally synchronizing the trajectories of a set of new chaos hyperjerk systems considered as *master–slave* systems.

The master hyperjerk system is taken as the new chaotic hyperjerk system

$$\begin{cases} \dot{x}_1 = y_1\,, \\ \dot{y}_1 = z_1\,, \\ \dot{z}_1 = w_1\,, \\ \dot{w}_1 = -x_1 - y_1 - pz_1 - w_1 - ax_1z_1 - bx_1y_1 - cy_1z_1 + qz_1^2\,. \end{cases} \tag{12}$$

We denote the state of the 4-D master hyperjerk system (12) as $X = (x_1, y_1, z_1, w_1)$.

The slave hyperjerk system is taken as the new controlled chaotic hyperjerk system

$$\begin{cases} \dot{x}_2 = y_2\,, \\ \dot{y}_2 = z_2\,, \\ \dot{z}_2 = w_2\,, \\ \dot{w}_2 = -x_2 - y_2 - pz_2 - w_2 - ax_2z_2 - bx_2y_2 - cy_2z_2 + qz_2^2 + v. \end{cases} \tag{13}$$

We denote the state of the 4-D slave hyperjerk system (13) as $Y = (x_2, y_2, z_2, w_2)$. Also, v is the active backstepping control which is to be determined using backstepping control theory.

The synchronization error between the master and slave hyperjerk systems is defined as follows:

$$\begin{cases} e_x = x_2 - x_1\,, \\ e_y = y_2 - y_1\,, \\ e_z = z_2 - z_1\,, \\ e_w = w_2 - w_1\,. \end{cases} \tag{14}$$

The synchronization error dynamics is calculated as follows:

$$\begin{cases} \dot{e}_x = e_y\,, \\ \dot{e}_y = e_z\,, \\ \dot{e}_z = e_w\,, \\ \dot{e}_w = -e_x - e_y - pe_z - e_w - a(x_2z_2 - x_1z_1) - b(x_2y_2 - x_1y_1) \\ \qquad - c(y_2z_2 - y_1z_1) + q\left(z_2^2 - z_1^2\right) + v. \end{cases} \tag{15}$$

We state and prove the main control result of this section.

Theorem 1. *The active backstepping control law stated by*

$$\begin{aligned} v = {} & -4e_x - 9e_y - (9-p)e_z - 3e_w - K\eta_4 + a(x_2z_2 - x_1z_1) \\ & + b(x_2y_2 - x_1y_1) + c(y_2z_2 - y_1z_1) - q(z_2^2 - z_1^2), \end{aligned} \tag{16}$$

where $K > 0$ and $\eta_4 = 3e_x + 5e_y + 3e_z + e_w$, globally and asymptotically synchronizes the trajectories of the 4D chaotic hyperjerk systems (12) and (13) for all values of $X(0),\ Y(0) \in \mathbb{R}^4$.

Proof. For the control design, we start with the Lyapunov function

$$V_1(\eta_x) = \frac{1}{2}\eta_1^2\,, \tag{17}$$

where

$$\eta_1 = e_x\,. \tag{18}$$

Differentiating V_1 with respect to t along the error system (15), we get

$$\dot{V}_1 = \eta_1\dot{\eta}_1 = -\eta_1^2 + \eta_1(e_x + e_y). \tag{19}$$

We define

$$\eta_2 = e_x + e_y\,. \tag{20}$$

Using (20), we simplify (19) as

$$\dot{V}_1 = -\eta_1^2 + \eta_1\eta_2\,. \tag{21}$$

We proceed next with defining the Lyapunov function

$$V_2(\eta_1, \eta_2) = V_1(\eta_1) + \frac{1}{2}\,\eta_2^2 = \frac{1}{2}\eta_1^2 + \frac{1}{2}\eta_2^2\,. \tag{22}$$

Differentiating V_2 with respect to t along the error system (15), we get

$$\dot{V}_2 = -\eta_x^2 - \eta_y^2 + \eta_y(2e_x + 2e_y + e_z). \tag{23}$$

We define

$$\eta_3 = 2e_x + 2e_y + e_z\,. \tag{24}$$

Using (24), we simplify (23) as

$$\dot{V}_2 = -\eta_1^2 - \eta_2^2 + \eta_2\eta_3\,. \tag{25}$$

Next, we define the Lyapunov function

$$V_3(\eta_1, \eta_2, \eta_3) = V_2(\eta_x, \eta_y) + \frac{1}{2}\,\eta_3^2 = \frac{1}{2}(\eta_1^2 + \eta_2^2 + \eta_3^2). \tag{26}$$

Differentiating V_3 with respect to t along the error system (15), we get

$$\dot{V}_3 = -\eta_1^2 - \eta_2^2 - \eta_3^2 + \eta_3(3e_x + 5e_y + 3e_z + e_w). \tag{27}$$

We define

$$\eta_4 = 3e_x + 5e_y + 3e_z + e_w\,. \tag{28}$$

Using (28), we simplify (27) as

$$\dot{V}_3 = -\eta_1^2 - \eta_2^2 - \eta_3^2 + \eta_4\eta_4\,. \tag{29}$$

Finally, we define the quadratic Lyapunov function

$$V(\eta_1, \eta_2, \eta_3, \eta_4) = V_3(\eta_1, \eta_2, \eta_3) + \frac{1}{2}\,e_4^2 = \frac{1}{2}\,e_1^2 + \frac{1}{2}\,e_2^2 + \frac{1}{2}\,e_3^2 + \frac{1}{2}\,e_4^2\,. \tag{30}$$

Differentiating V with respect to t, we get

$$\dot{V} = -\eta_1^2 - \eta_2^2 - \eta_3^2 - \eta_4^2 + \eta_4 Q, \tag{31}$$

where

$$Q = \eta_3 + \eta_4 + \dot{\eta}_4 \,. \tag{32}$$

Simplifying the expression in (32), we get

$$\begin{aligned} Q = {} & 4e_x + 9e_y + (9-p)e_z + 3e_w - a(x_2z_2 - x_1z_1) \\ & - b(x_2y_2 - x_1y_1) - c(y_2z_2 - y_1z_1) + q(z_2^2 - z_1^2) + v. \end{aligned} \tag{33}$$

Substituting v from Eq. (16) into (33), we get

$$Q = -K\eta_4 \,. \tag{34}$$

Using (34) and (31), we get

$$\dot{V} = -\eta_1^2 - \eta_2^2 - \eta_3^2 - (1+K)\eta_4^2 \,. \tag{35}$$

From (35), $\dot{V}$ is negative definite on $\mathbb{R}^4$.

Consequently, by Lyapunov stability theory, $(e_x(t), e_y(t), e_z(t), e_w(t)) \to 0$ as $t \to \infty$ for all values of the initial conditions $X(0), Y(0) \in \mathbb{R}^4$. □

For computer simulations, we take the parameter values as in the chaos case, *viz.* $a = 0.3$, $b = 0.2$, $c = 0.4$, $p = 0.2$ and $q = 0.2$.

We choose the feedback gain K as $K = 20$.

We take $X(0) = (1.6, 4.3, 7.2, 3.9)$ and $Y(0) = (2.8, 1.5, 3.1, 8.6)$.

Figure 10 shows the asymptotic convergence of the synchronization error $e_x(t)$, $e_y(t)$, $e_z(t)$ and $e_w(t)$ between the master system (12) and the slave system (13).

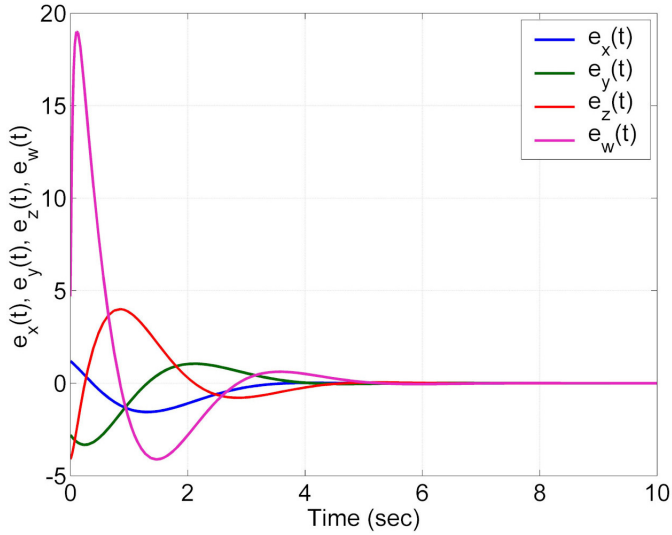

Figure 10: Time-plot of the synchronization errors between the master system (12) and the slave system (13)

7. Conclusions

In this research work, we described a new four-dimensional chaotic hyperjerk system with four quadratic nonlinearities. We performed a detailed bifurcation analysis and derive conditions for the existence of a Hopf bifurcation for the new hyperjerk system. A linear stability analysis of the 4-D hyperjerk system gives a unique trivial equilibrium state, whose stability depends only upon the parameter p. We showed that the only simple bifurcations possible are a Hopf bifurcation when $p = 2$, with the remaining two eigenvalues having negative real parts. We noted that the Hopf bifurcation is supercritical and that the bifurcation transition diagrams as p varies clearly verify this Hopf bifurcation, as well as period-halving bifurcations. We showed phase portraits of the new hyperjerk system in the (x, y)-space of examples of a period-1, period-2, period-4 orbit in the bifurcation sequence, as well as a broad-banded period-5 example in a periodic window. The dynamics at the chosen value of $p = 0.2$ is well inside the chaotic region. Next, we derived new results for the new chaotic hyperjerk system showing multistability and the existence of coexisting attractors for the new chaotic hyperjerk system. Using MultiSim, a new electronic circuit was designed for the new chaotic hyperjerk system with four quadratic nonlinearities. Finally, we presented a control application for the proposed chaotic hyperjerk system with four quadratic nonlinearities. Using active backstepping control and Lyapunov stability theory, we designed a new controller that achieves complete synchronization for the master-slave chaotic hyperjerk systems with four quadratic nonlinearities. A numerical example was presented to illustrate the complete synchronization for the new chaotic hyperjerk systems taken as the master-slave systems.

References

[1] E. Abbasi and S. Jafari: Chaotic dynamics in X-ray free-electron lasers with an optical undulator. *Scientific Reports*, **14**(1), (2024). DOI: 10.1038/s41598-024-51891-1

[2] H. Liu, G. Dong, T. Zhao, X. Chen, J. Yu and M. Zhang: Monitoring distance enhancement with chaotic laser for OTDR system. *IEEE Sensors Journal*, **24**(3), (2024), 2822–2827. DOI: 10.1109/JSEN.2023.3340181

[3] sc V. Rybin, D. Butusov, I. Babkin, D. Pesterev and V. Arlyapov: Some properties of a discrete Lorenz system obtained by variable midpoint method and its application to chaotic signal modulation. *International Journal of Bifurcation and Chaos*, **34**(1), (2024). DOI: 10.1142/S0218127424500093

[4] L. Shen and K. Shen: Skyrmion-based chaotic oscillator driven by a constant current. *Physical Review B*, **109**(1), (2024). DOI: 10.1103/PhysRevB.109.014422

[5] F. Wang, Z. Wu and T. Bao: Time-jerk optimal trajectory planning of industrial robots based on a hybrid WOA-GA algorithm. *Processes*, **10**(5), (2022). DOI: 10.3390/pr10051014

[6] Z. Liu, J. Gao, X. Rao, S. Ding and D. Liu: Complex dynamics of the passive biped robot with flat feet: Gait bifurcation, intermittency and crisis. *Mechanism and Machine Theory*, **191** (2024). DOI: 10.1016/j.mechmachtheory.2023.105500

[7] Y. Li, C. Li, Q. Zhong, S. Liu and T. Lei: A memristive chaotic map with only one bifurcation parameter. *Nonlinear Dynamics*, **112**(5), (2024), 3869–3886. DOI: 10.1007/s11071-023-09204-0

[8] X. An, S. Liu, L. Xiong, J. Zhang and X. Li: Mixed gray-color images encryption algorithm based on a memristor chaotic system and 2D compression sensing. *Expert Systems with Applications*, **243** (2024). DOI: 10.1016/j.eswa.2023.122899

[9] H. Wen and Y. Lin: Cryptanalysis of an image encryption algorithm using quantum chaotic map and DNA coding. *Expert Systems with Applications*, **237** (2024). DOI: 10.1016/j.eswa.2023.121514

[10] A.Y. Darani, Y.K. Yengeyeh, H. Pakmanesh and G. Navarro: Image encryption algorithm based on a new 3D chaotic system using cellular automata. *Chaos, Solitons and Fractals*, **179** (2024). DOI: 10.1016/j.chaos.2023.114396

[11] M.D. Johansyah, A. Sambas, S. Qureshi, S. Zheng, T.M. Abed-Elhameed, S. Vaidyanathan and I.M. Sulaiman: Investigation of the hyperchaos and control in the fractional order financial system with profit margin. *Partial Differential Equations in Applied Mathematics*, **9** (2024). DOI: 10.1016/j.padiff.2023.100612

[12] K.B. Kacchia: Chaos in fractional order financial model with fractal–fractional derivatives. *Partial Differential Equations in Applied Mathematics*, **7** (2023). DOI: 10.1016/j.padiff.2023.100502

[13] A. Sambas, M. Mahdal, S. Vaidyanathan, B. Ovilla-Martinez, E. Tlelo-Cuautle, A.A.A. El-Latif, B. Abd-El-Atty, K. Benkouider and T. Bonny: A new hyperjerk system with a half line equilibrium: Multistability, period doubling reversals, antimonotonocity, electronic circuit, FPGA design, and an application to image encryption. *IEEE Access*, **12** (2024), 9177–9194. DOI: 10.1109/ACCESS.2024.3351693

[14] E. Zambrano-Serrano and A. Anzo-Hernandez: A novel antimonotic hyperjerk system: Analysis, synchronization and circuit design. *Physica D: Nonlinear Phenomena*, **424** (2021). DOI: 10.1016/j.physd.2021.132927

[15] R. Wang, C. Li, S. Cicek, K. Rajagopal and X. Zhang: A memristive hyperjerk chaotic system: Amplitude control, FPGA design, and prediction with artificial neural network. *Complexity*, **2021** (2021). DOI: 10.1155/2021/6636813

[16] L. Moysis, E. Petavratzis, M. Marwan, C. Volos, H. Nistazakis and S. Ahmad: Analysis, synchronization, and robotic application of a modified hyperjerk chaotic system. *Complexity*, **2020** (2020). DOI: 10.1155/2020/2826850

[17] L.G. Costa and M.A. Savi: Nonlinear dynamics of a compact and multistable mechanical energy harvester. *International Journal of Mechanical Sciences*, **262** (2024). DOI: 10.1016/j.ijmecsci.2023.108731

[18] L. Laskaridis, C. Volos, H. Nistazakis and E. Meletlidou: Exploring the dynamics of a multistable general model of discrete memristor-based map featuring an exponentially varying memristance. *Integration*, **95** (2024). DOI: 10.1016/j.vlsi.2023.102131

[19] S. Shi, C. Du and L. Liu: Complex dynamics analysis and feedback control for a memristive switched chaotic system. *Physica Scripta*, **98**(12), (2023). DOI: 10.1088/1402-4896/ad03cb

[20] V.-T. Pham, S. Vaidyanathan, C. Volos, S. Jafari and S.T. Kingni: A no-equilibrium hyperchaotic system with a cubic nonlinear term. *Optik*, **127** (2016), 3259–3265. DOI: 10.1016/j.ijleo.2015.12.048